Selectivity of the Yersiniabactin Synthetase Adenylation Domain in the Two-Step Process of Amino Acid Activation and Transfer to a Holo-Carrier Protein Domain†

Thomas A. Keating, Zucai Suo, David E. Ehmann, and Christopher T. Walsh*

Department of Biological Chemistry and Molecular Pharmacology, Harvard Medical School, Boston, Massachusetts 02115

Received October 7, 1999; Revised Manuscript Received December 14, 1999

ABSTRACT: The adenylation (A) domain of the *Yersinia pestis* nonribosomal peptide synthetase that biosynthesizes the siderophore yersiniabactin (Ybt) activates three molecules of L-cysteine and covalently aminoacylates the phosphopantetheinyl (P-pant) thiols on three peptidyl carrier protein (PCP) domains embedded in the two synthetase subunits, two *in cis* (PCP1, PCP2) in subunit HMWP2 and one *in trans* (PCP3) in subunit HMWP1. This two-step process of activation and loading by the A domain is analogous to the operation of the aminoacyl-tRNA synthetases in ribosomal peptide synthesis. Adenylation domain specificity for the first step of reversible aminoacyl adenylate formation was assessed with the amino acid-dependent [^{32}P]-PP$_i$−ATP exchange assay to show that *S*-2-aminobutyrate and β-chloro-L-alanine were alternate substrates. The second step of A domain catalysis, capture of the bound aminoacyl adenylate by the P-pant-SH of the PCP domains, was assayed both by catalytic release of PP$_i$ and by covalent aminoacylation of radiolabeled substrates on either the PCP1 fragment of HMWP2 or the PCP3-thioesterase double domain fragment of HMWP1. There was little selectivity for capture of each of the three adenylates by PCP3 in the second step, arguing against any hydrolytic proofreading of incorrect substrates by the A domain. The holo-PCP3 domain accelerated PP$_i$ release and catalytic turnover by 100−200-fold over the leak rate (<1 min^{-1}) of aminoacyl adenylates into solution while PCP1 *in trans* had only about a 5-fold effect. Free pantetheine could capture cysteinyl adenylate with a 25−50-fold increase in k_{cat} while CoA was 10-fold less effective. The K_m of free pantetheine (30−50 mM) was 3 orders of magnitude larger than that of PCP3-TE (10−25 μM), indicating a net 10^4 greater catalytic efficiency for transfer to the P-pant arm of PCP3 by the Ybt synthetase A domain, relative to P-pant alone.

Nonribosomal peptide synthetases (NRPSs)[1] (*1*−*3*) are large, multifunctional, multidomain proteins or protein complexes that biosynthesize many medicinally important compounds [bacitracin (*4*), penicillin (*5*), vancomycins (*6*)] as well as a number of iron-chelating bacterial virulence factors, among them enterobactin from *E. coli* (*7*), mycobactin from *M. tuberculosis* (*8*), pyochelin from *P. aeruginosa* (*9*), and yersiniabactin from *Y. pestis* (Figure 1A) (*10*). We have been studying this last compound, a siderophore from the plague-causing bacterium, and its nonribosomal synthesis by three proteins, YbtE, HMWP2, and HMWP1 (Figure 1B).

From study of both the yersiniabactin structure and the domain organization of the three proteins, we have predicted that yersiniabactin is assembled from salicylic acid, three cysteines (cyclized to form two thiazolines and a thiazolidine), and malonic acid. Methylation and an imine reduction complete the necessary chemical steps (*10*). Thus far, we have managed to express large, functional fragments of HMWP2 and have demonstrated that these fragments can synthesize both the first thiazoline ring (*11*) as well as the first two as the bisheterocycle (*12*).

NRPSs follow the thiotemplated model for peptide synthesis (*13*). In this model, carrier protein domains are first posttranslationally modified by attachment of a coenzyme A-derived phosphopantetheine to a specific serine side chain in the carrier protein domain by a dedicated phosphopantetheinyl transferase (PPTase) (*14*). The resulting free thiol is then aminoacylated with the correct amino acid monomer by an adenylation (A) domain. Biosynthesis then proceeds along the synthetase in the N-to-C direction, with interspersed condensation (C) or cyclization (Cy) domains responsible for linking downstream monomers to the growing, upstream chain, each tethered through a thioester bond to the carrier protein domains (*15*).

Of principal importance to the understanding of NRPSs is the nature of their selectivity and specificity that results in efficient [$\sim$100 min^{-1} for enterobactin (*7*)] production of the specific product of correct sequence. Not only is an understanding of NRPS specificity important in studying the natural systems, but with growing interest in constructing novel NRPSs for "combinatorial biosynthesis" (*16*), such an

† This work has been supported by the National Institutes of Health (Grant GM20011 to C.T.W.). T.A.K. is a Fellow of the Cancer Research Fund of the Damon Runyon−Walter Winchell Foundation (DRG-1483). Z.S. is a Fellow of the Jane Coffin Childs Memorial Fund for Medical Research. D.E.E. is a National Science Foundation Predoctoral Fellow.

* To whom correspondence should be addressed. Phone: 617-432-1715; fax: 617-432-0438; email: walsh@walsh.med.harvard.edu.

[1] Abbreviations: NRPS, nonribosomal peptide synthetase; HMWP, high molecular weight protein; CoA, coenzyme A; A, adenylation domain; PPTase, phosphopantetheinyl transferase; P-pant, 4′-phosphopantetheine; ACV, δ-(L-α-aminoadipoyl)-L-cysteinyl-D-valine; AARS, aminoacyl-tRNA synthetase; PP$_i$, inorganic pyrophosphate; PCP, peptidyl carrier protein domain; TE, thioesterase domain; PNP, calf spleen purine nucleoside phosphorylase; PP$_i$-ase, bakers' yeast inorganic pyrophosphatase; MESG, 2-amino-6-mercapto-7-methylpurine ribonucleoside; DTT, dithiothreitol; TCEP, tris(carboxyethyl)phosphine.

10.1021/bi992341z CCC: $19.00
Published on Web 02/10/2000

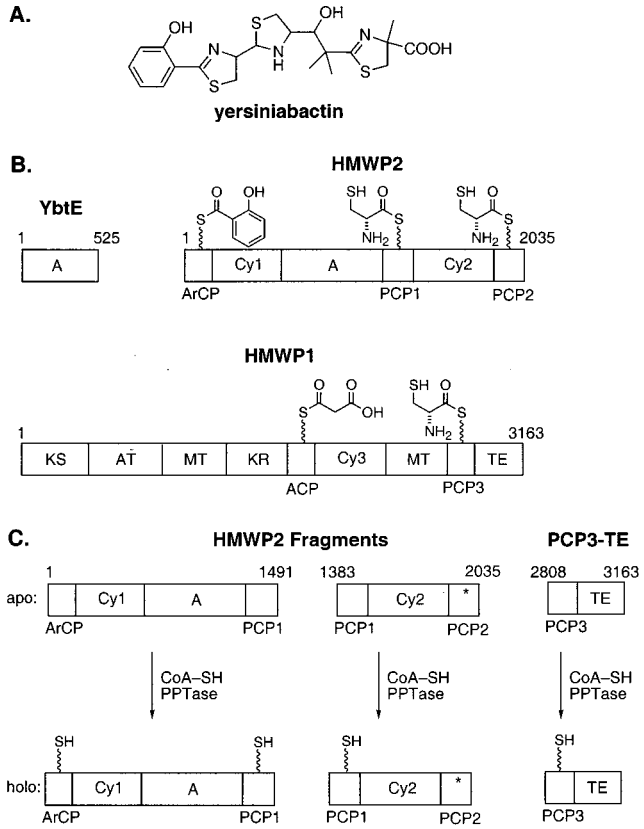

FIGURE 1: (A) Structure of yersiniabactin (Ybt). (B) Domain organization of the three proteins of yersiniabactin synthetase: YbtE, HMWP2, and HMWP1. (A = adenylation, ArCP = aryl carrier protein, Cy = cyclization, PCP = peptidyl carrier protein, KS = β-ketoacyl synthase, AT = acyltransferase, MT = methyltransferase, KR = ketoreductase, ACP = acyl carrier protein, TE = thioesterase.) Numbers indicate amino acid residues. Each carrier protein domain is depicted with the appropriate monomer thioesterified to its posttranslationally introduced phosphopantetheine (P-pant) tether. (C) Ybt synthetase fragments used in this study, and the process of posttranslational introduction of the P-pant prosthetic arm by a phosphopantetheinyl transferase (PPTase) and coenzyme A. The asterisk indicates Ser1977Ala mutation that prevents P-pant attachment to the PCP2 domain.

understanding is essential for creating unnatural systems. The adenylation domains must select the appropriate amino acid monomer from the cellular pool, activate it with ATP, and transfer the enzyme-bound, activated species to the phosphopantetheine thiol of the correct carrier protein domain. This two-step process is similar and analogous to the aminoacylation of tRNAs by aminoacyl-tRNA synthetases (AARS) that occurs in ribosomal peptide synthesis.

A diagram of these two pathways is shown in Figure 2. In each case, the first step entails binding of an amino acid and ATP by the enzyme (adenylation domain or AARS), activation of the amino acid as the mixed anhydride with AMP, and release of inorganic pyrophosphate (PP_i). The enzyme retains the labile aminoacyl-AMP in its active site, and, in the second step, binds the acceptor species [a peptidyl carrier protein domain (PCP) or a tRNA] and transfers the aminoacyl group to a nucleophilic sulfur (PCP) or oxygen (tRNA). Upon release of the acceptor, the A domain is emptied, and the cycle can begin again.

The specificity of aminoacyl-tRNA synthetases toward amino acids and tRNAs has been well studied, while the corresponding studies of NRPSs are ongoing (*17*). Both kinds

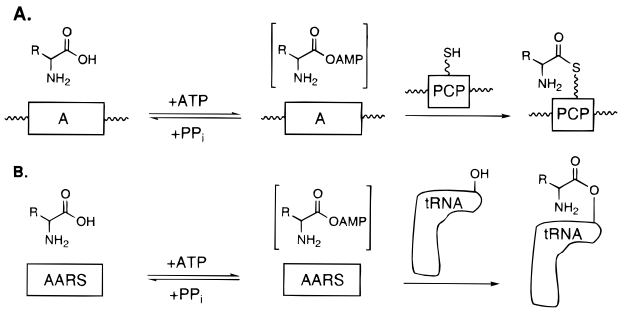

FIGURE 2: Comparison of the analogous two-step processes of amino acid activation and transfer by NRPS adenylation domains and aminoacyl-tRNA synthetases (AARS). (A) The A domain first activates a specific amino acid in an ATP-dependent manner as the enzyme-bound aminoacyl adenylate. A holo-PCP domain is then aminoacylated on its P-pant thiol. Although the PCP is depicted as a separate protein fragment, the most common NRPS architecture has the PCP fused immediately downstream of its paired A domain. (B) The AARS also activates a specific amino acid as the aminoacyl adenylate, but transfers the activated species to a hydroxyl group of its cognate tRNA.

of activating domains have typically been assayed by amino acid-dependent [^{32}P]-pyrophosphate exchange into ATP, an assay used extensively to probe selectivity of AARS (*18*). Classically, this exchange assay has been utilized not only to show selectivity in aminoacyl-AMP formation by AARS but also as the first step in establishment of hydrolytic editing and double sieving proposals to account for error-correcting and fidelity-checking steps detected in some AARS (*18*). The PP_i−ATP exchange, however, measures only the first stage of A domain action, up to and including reversible formation of aminoacyl-AMP in the A domains' active sites, but not the second catalytic step involving transfer of the activated aminoacyl group onto a nucleophilic cosubstrate. In contrast to the tRNA synthetases where the cosubstrate tRNA is a diffusable substrate and the aa-tRNA a releasable, soluble coproduct, the cognate step in NRPS domain catalytic action is typically an intramolecular, stoichiometric self-acylation of an adjacent PCP and thus is more difficult to evaluate for specificity and rate of transfer. It has remained unclear whether there is any selectivity or editing in the second step of A domain function by nonribosomal peptide synthetases, either for hydrolytic correction of aminoacyl adenylates or for aminoacyl-*S*-PCP misacylations, in analogy to two proofreading mechanisms of AARSs (*19, 20*).

In this study, we address subunits 1 and 2, known perversely as HMWP2 and HMWP1 (HMWP = high molecular weight protein), respectively, of yersiniabactin (Ybt) synthetase. In an unusual NRPS organization in this assembly line, there is only a single A domain, L-cysteine-specific, that services three PCP domains, known as PCP1, PCP2, and PCP3, that act as the thiol waystations for the three cysteine monomers that are precursors to the three thiazoline/thiazolidine heterocycles in the siderophore. Two of the PCP domains (PCP1 and PCP2 in subunit HMWP2) are *in cis* while the third is *in trans* (PCP3 in subunit HMWP1) to the A domain. We have directly assayed the Ybt A domain, expressed conveniently in the 1−1491 residue fragment of HMWP2 (*11*), for specificity both in the amino acid-activating first half-reaction and in the aminoacyl-AMP transfer to several pantetheinyl thiol groups in the second half-reaction. This second half-reaction is assayable both by transfer of a radioactive amino acid into covalent acyl-*S*-

PCP attachment and also by a continuous PP_i release assay. Since aminoacyl-AMPs are tightly sequestered in A domain active sites in the absence of specific thiol nucleophilic cosubstrates, the acceleration of PP_i release by holo-PCPs allows distinction between specific aminoacyl-*S*-PCP formation and slow, adventitious capture of aa-AMP molecules that have "leaked" from A domains into solution.

EXPERIMENTAL PROCEDURES

Reagents. *S*-2-Aminobutyric acid, β-chloro-L-alanine, pantethine, coenzyme A, L-cysteine, and ATP were purchased from Sigma/Aldrich. [1-^{14}C]-L/D-2-Aminobutyric acid (15.6 mM, 7.6 Ci/mol) was purchased from ICN. [^{35}S]-L-Cysteine (10 μM, 1075 Ci/mmol) and sodium [^{32}P]-pyrophosphate (534 μM, 19 Ci/mmol) were purchased from NEN. Pantetheine stocks were prepared by reducing pantethine with 1.5 equiv of tris(carboxyethyl)phosphine (TCEP). 2-Amino-6-mercapto-7-methylpurine ribonucleoside (MESG) was synthesized from 2-amino-6-chloropurine ribonucleoside according to published procedures (*21*). The UV absorbance spectrum of synthesized MESG was identical to a published spectrum (*21*). Phosphate-free, calf spleen purine nucleoside phosphorylase (PNP) and bakers' yeast inorganic pyrophosphatase (PP_i-ase) were purchased lyophilized from Sigma and stored as 0.01 unit/μL stocks in 75 mM Tris, pH 7.5, 10 mM $MgCl_2$. Sfp, a phosphopantetheinyl transferase from *Bacillus subtilis*, has been described previously (*22*) and was a gift from Luis E. N. Quadri. EntD, a phosphopantetheinyl transferase from *E. coli*, has also been described previously (*14*). Competent *E. coli* strain BL21(DE3) and the pET22b expression vector were purchased from Novagen. Competent *E. coli* strain DH5α was purchased from GibcoBRL. Restriction endonucleases and T4 DNA ligases were obtained from New England Biolabs. *Pfu* DNA polymerase was purchased from Stratagene.

Methods. Standard recombinant DNA techniques were performed as described (*23*). Preparation of plasmid DNA, gel purification of DNA fragments, and purification of PCR products were performed using QIAprep plasmid miniprep kits, QIAquick gel extraction kits, and QIAquick DNA purification kits, respectively (Qiagen). PCRs were carried out with *Pfu* polymerase, according to its supplier's instructions. Oligonucleotide primers were purchased from Integrated DNA Technologies, and DNA sequencing was performed on double-stranded DNA by the Molecular Biology Core Facilities of the Dana-Farber Cancer Institute (Boston, MA).

HMWP2 1−*1491.* The cloning, overexpression, and purification of the 1−1491 amino acid fragment of HMWP2 have been described previously (*11*). This fragment includes the domains ArCP-Cy1-A-PCP1. HMWP2 1−1491 bears a hexahistidine affinity tag at its C-terminus.

HMWP2 1383−*2035 (S1977A).* The cloning, overexpression, and purification of the 1383−2035 fragment of HMWP2, with a Ser to Ala mutation at position 1977 have been described previously (*12*). This fragment includes the domains PCP1-Cy2-PCP2, with PCP2 inactivated by mutation of Ser1977, the point of phosphopantetheine attachment, to Ala. HMWP2 1383−2035 (S1977A) has a hexahistidine tag at its C-terminus.

Cloning, Overexpression, and Purification of PCP3-TE. The *Y. pestis irp1* gene fragment corresponding to the 40.3 kDa C-terminal 356 amino acids of HMWP1 (residues 2808−3163) was amplified from pSDR498.4 (Robert D. Perry, unpublished plasmid) by PCR, employing the forward primer 5′-GAATTCCATATGGCCCCGTCTGATGCGCC and the reverse primer 5′-CCACCGCTCGAGTAACGTGT-TCTCCGGTTGCGTTG. After restriction digestion, this PCR product was ligated to the *Nde*I/*Xho*I sites (underlined above) of pET22b to give pET22b-PCP3TE. This plasmid directs production of PCP3-TE as a histidine tag fusion with amino acid sequence LEHHHHHH appended to the C-terminus. The fidelity of the pET22b-PCP3TE insert was confirmed by DNA sequencing.

For overexpression and purification of apo-PCP3-TE, cultures of *E. coli* strain BL21(DE3) transformed with pET22b-PCP3TE (2 × YT media, 50 μg/mL ampicillin) were grown at 37 °C to an optical density (600 nm) of 0.7 and then induced with 1 mM isopropyl-D-thiogalactopyranoside (IPTG) and incubated at 15 °C. Cells were harvested after 4 h, and the cell paste was resuspended in buffer A (20 mM Tris-Cl, pH 7.9, 0.5 M NaCl). Cells were lysed by passage through a French pressure cell at 15 000 psi twice, and the lysate was clarified by centrifugation (95000*g*) for 30 min. Protein was purified from the lysate by nickel chelation chromatography over 4 mL of Ni−NTA superflow resin (Qiagen). Fractions containing protein were determined by SDS−polyacrylamide gel electrophoresis (SDS−PAGE) and then pooled and dialyzed against 50 mM Tris-HCl, pH 8.0, 2 mM DTT, 10 mM $MgCl_2$, 0.1 mM EDTA, and 10% glycerol. Concentration of the purified apo-PCP3-TE was determined spectrophotometrically at 280 nm using the calculated extinction coefficient of 58 690 $(M\cdot cm)^{-1}$. The yield after purification was 3 mg/L.

Overexpression and purification of holo-PCP3-TE followed the above procedures except that *E. coli* strain BL21(DE3) was transformed with both pET22b-PCP3TE and pREP4-Sfp (Mohamed A. Marahiel, unpublished plasmid). The plasmid pREP4-Sfp was derived from pREP4 (Qiagen) by insertion of the *sfp* gene (PPTase from *Bacillus subtilis*). Cultures of this *E. coli* strain after IPTG induction coexpressed apo-PCP3-TE and Sfp, and the purified PCP3-TE is thus obtained in holo-form since apo-PCP3TE was modified by coexpressed Sfp in vivo. Complete phosphopantetheinylation was verified by attempted incorporation of [^{3}H]-coenzyme A into holo-PCP3-TE by Sfp in vitro, and by mass spectrometry (MALDI-TOF and electrospray ionization methods) of PCP3-TE.

ATP−*PP_i Exchange Reactions.* Reactions were carried out at 30 °C in 100 μL total volume and contained 75 mM Tris, pH 7.5, 10 mM $MgCl_2$, 5 mM DTT, 3 mM ATP, 150 nM HMWP2 1−1491, 1 mM [^{32}P]-pyrophosphate, and varying concentrations of amino acid substrate. The reactions were initiated by addition of [^{32}P]-pyrophosphate, allowed to proceed for 6−8 min, and then quenched by addition of a charcoal−pyrophosphate−perchloric acid mixture [1.6% (w/v) activated charcoal, 4.46% (w/v) tetrasodium pyrophosphate, 3.5% perchloric acid in water]. The charcoal was then pelleted by centrifugation, washed twice with the quench mixture without added charcoal, and then resuspended in 0.5 mL of water and submitted for liquid scintillation counting. Reactions were typically performed in duplicate. The amount of bound radioactivity was converted into reaction velocity using the specific activity of the [^{32}P]-pyrophosphate. The

velocity was plotted against substrate concentration and fit to the Michaelis−Menten equation.

Amino Acid-Dependent ATP Usage by Apo-HMWP2 1−1491. A coupled, continuous, spectrophotometric assay for inorganic pyrophosphate was employed (*24*−*26*). Reactions were carried out at 30 °C in 150 μL total volume in a quartz cuvette and contained 75 mM Tris, pH 7.5, 10 mM $MgCl_2$, 200 μM MESG, 0.15 unit of PNP, 0.15 unit of PP_i-ase, 2 mM ATP, either 5 mM L-Cys or 10 mM β-Cl-L-Ala or 10 mM *S*-2-aminobutyrate, and varying concentrations of HMWP2 1−1491. Reactions were initiated by addition of the amino acid substrate after a 10 min incubation to allow the PP_i-ase/PNP/MESG couple to remove any contaminating PP_i or P_i. A Perkin-Elmer Lambda 6 spectrophotometer was used to monitor absorbance at 360 nm and compute rates of A_{360} increase. The spectrophotometer recorded data points every 6 s, and a minimum of eight collinear data points, representing a linear reaction velocity, were used to calculate a slope. Substrate-specific pyrophosphate release was measured by subtracting the rate of A_{360} increase before amino acid addition from the A_{360} rate after addition. This net rate was converted to reaction velocity through the molar extinction coefficient (ϵ) of MESG. The molar extinction coefficient was obtained from a standard curve constructed from known pyrophosphate concentrations added to the assay mixture described above plotted against A_{360}. This plot was linear between 0 and 24 μM pyrophosphate, and yielded $\epsilon = 17\,600\ (M \cdot cm)^{-1}$. At least three velocities measured at different HMWP2 1−1491 concentrations were averaged to obtain a final velocity.

Amino Acid-Dependent ATP Usage by Holo-HMWP2 1−1491. Reactions were performed as above except reactions contained in addition 67 μM coenzyme A and 133 nM Sfp and were incubated for 20 min at 25 °C for allow for phosphopantetheinylation before reaction initiation. These reactions were also performed in the absence or presence (5 mM) of DTT to examine effects of added thiols.

Transfer of Activated Amino Acids to Acceptor Substrates. The same continuous assay was employed to measure the kinetics of amino acid transfer from HMWP2 1−1491 to a variety of acceptor cosubstrates: holo-PCP3-TE, holo-HMWP2 1383−2035 (S1977A), CoA, and pantetheine. Reactions were performed at 30 °C in 150 μL total volume and contained 75 mM Tris, pH 7.5, 10 mM $MgCl_2$, 200 μM MESG, 0.15 unit of PNP, 0.15 unit of PP_i-ase, 2 mM ATP, 75−620 nM HMWP2 1−1491, either 5 mM L-Cys or 10 mM β-Cl-L-Ala or 10 mM *S*-2-aminobutyrate, and varying concentrations of acceptor cosubstrate. CoA (100 μM) and Sfp (133 nM) were added to HMWP2 1382−2035 (S1977A) reactions to convert apo- to holo-substrate. Reactions were initiated by amino acid addition, and initial velocities were computed as described above. Plotting of these velocities against acceptor cosubstrate concentration was followed by fitting to the Michaelis−Menten equation.

Second, a radioactive incorporation assay was used to measure rates of precipitable [^{35}S]-L-Cys transferred from HMWP2 1−1491 to PCP3-TE. Two different experiments were performed. In the first, 50 μL reactions contained 75 mM Tris, pH 8.0, 10 mM $MgCl_2$, 5 mM DTT, 1 mM CoA, 550 nM EntD, 150 nM HMWP2 1−1491, 100 μM [^{35}S]-L-Cys (1.2 Ci/mmol), 5 mM ATP, and varying amounts of apo-PCP3-TE. Phosphopantetheinylation was allowed to proceed for 30 min at 37 °C before initiation by ATP addition. Reactions were quenched after 45 s with 0.8 mL of 10% trichloroacetic acid (TCA). The precipitated protein was pelleted and washed twice with fresh 10% TCA. The pellet was redissolved in 150 μL of 88% formic acid and submitted for liquid scintillation counting. Kinetic parameters were calculated as for the ATP−PP_i reaction. In the second experiment, holo-PCP3-TE was employed in 75 mM Tris, pH 7.5, 10 mM $MgCl_2$, 1 mM TCEP, 20 nM apo-HMWP2 1−1491, 2 mM ATP, 100 μM [^{35}S]-L-Cys under otherwise identical conditions.

Stoichiometries of Covalent Aminoacylation of Holo-PCP3-TE and HMWP2 1383−2035 (S1977A). To determine the extent of conversion of PCP3 and PCP1 to their aminoacylated forms by the adenylation domain acting *in trans*, incorporation of [^{35}S]-L-Cys and [1-^{14}C]-L/D-2-aminobutyric acid was measured. Reactions (100 μL) contained 75 mM, Tris pH 7.5, 10 mM $MgCl_2$, 1 mM TCEP, 310 nM apo-HMWP2 1−1491, 5 μM PCP substrate, 5 mM ATP, and 250 μM [^{35}S]-L-Cys or 312 μM [1-^{14}C]-L/D-2-aminobutyric acid. HMWP2 1383−2035 (S1977A) reactions contained in addition 100 μM CoA and 133 nM Sfp and were allowed to incubate at room temperature for 30 min to ensure phosphopantetheinylation prior to labeled amino acid addition. As a further check on the extent of in vivo phosphopantetheinylation of PCP3-TE, an identical set of reactions was performed with the addition of 100 μM CoA and 133 nM Sfp. All reactions were incubated at 30 °C for 90 min before workup as above for the radioactive incorporation assay. Percent modification of PCP1 and PCP3 was calculated from the specific activity of the amino acid used and the concentrations of the protein substrates.

RESULTS

PCP3-TE Subcloning, Overexpression, and Purification. The 40.3 kDa, two-domain PCP3-TE protein fragment represents the C-terminal 356 amino acids (2808−3163) of HMWP1. It contains the third carrier protein domain PCP3 (∼10 kDa), which is the attachment point for the third cysteine of yersiniabactin, plus the final domain (∼30 kDa), a thioesterase presumed to be responsible for release of the acyl chain of the mature siderophore from a thioester linkage at PCP3. Amplification of the 1068 bp gene fragment from pSDR498.4 and subcloning in a pET22b overexpression plasmid yielded pET22b-PCP3TE. Overexpression in *E. coli* strain BL21(DE3) at 15 °C resulted in a final yield of 3 mg/L. Purification was based on C-terminal hexahistidine tag binding to Ni-charged resin.

Either apo-PCP3-TE could be converted to holo-PCP3-TE by in vitro phosphopantetheinylation with CoA and the PPTase Sfp or, preferably, holo-PCP3-TE was prepared in vivo by coexpression. Plasmid pET22b-PCP3TE was cotransformed into strain BL21(DE3) with pREP4-Sfp, which carries the PPTase gene *sfp*. This overexpression strain was grown and the protein purified as above for apo-PCP3-TE. The stoichiometry of phosphopantetheinylation was confirmed by subsequent phosphopantetheinylation in vitro by Sfp and [^{3}H]-CoA, and by MALDI-TOF and electrospray mass spectrometry. All experiments revealed no detectable apo-PCP3-TE (data not shown). Additionally, we compared the level of [^{35}S]-L-Cys and [1-^{14}C]-L/D-2-aminobutyric acid

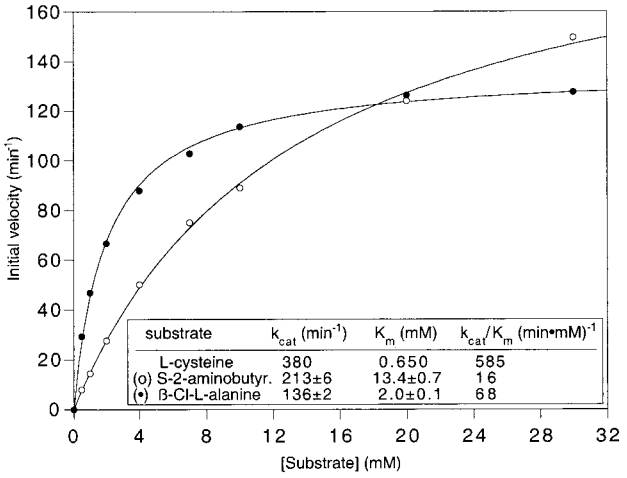

FIGURE 3: Amino acid-dependent ATP−PP_i exchange kinetics for HMWP2 1−1491 with *S*-2-aminobutyrate and *β*-chloro-L-alanine. Data for the natural substrate L-Cys were measured previously (*11*) and are shown for comparison.

incorporation both with and without additional, in vitro phosphopantetheinyltion with CoA and Sfp. We measured stoichiometries of 32% and 33% for [1-^{14}C]-L/D-2-aminobutyric acid incorporation without and with in vitro phosphopantetheinylation, respectively. The corresponding stoichiometries for [^{35}S]-L-Cys were 21% and 20%.

ATP−PP$_i$ Exchange Reactions of the Ybt Synthetase A Domain. To assess the adenylation domain specificity in the first step of amino acid activation, a number of natural and unnatural amino acids were employed as substrates in the ATP−PP_i exchange reaction as catalyzed by HMWP2 1−1491. In addition to the natural substrate L-cysteine, three other amino acids gave a positive signal: *S*-2-aminobutyric acid, *β*-chloro-L-alanine, and (very weakly) L-serine, while D-cysteine, *β*-fluoro-L/D-alanine, L-vinylglycine, L/D-allylglycine, 2,3-diaminopropionic acid, *O*-methyl-L/D-serine, 3-mercaptopropionic acid, thiolactic acid, and L/D-isoserine were all inactive. The kinetics for cysteine-dependent ATP−PP_i exchange have been measured previously (*11*), so *S*-2-aminobutyrate and *β*-chloro-L-alanine were subjected to the same set of experiments, while L-serine was not pursued further. The data are shown in Figure 3. While the catalytic efficiency for activation of the two substrates is down, approximately 40-fold and 10-fold respectively, from that of cysteine, the exchange reaction was still robust. For *S*-2-aminobutyrate, this decrease in catalytic efficiency represents a 2-fold decrease in k_{cat} and a 20-fold increase in K_m. Likewise, for *β*-chloro-L-alanine, we observed a 3-fold decrease in k_{cat} and a 3-fold increase in K_m. Since the k_{cat} for this exchange process includes both forward steps and back-reaction of [^{32}P]-PP_i with the aa-AMP, it is unclear if the close correspondence in k_{cat} reflects some common rate-determining step (e.g., pyrophosphate release rate). Neither of these amino acids is proteinogenic, and thus neither is expected to present significant in vivo competition for L-cysteine in A domain activation.

Amino Acid-Dependent ATP Consumption by Apo-HMWP2 1−1491. A continuous, coupled spectrophotometric assay was used to measure ATP usage by HMWP2 1−1491 (eq 1). This assay employs inorganic pyrophosphatase to hydrolyze PP_i (resulting from ATP cleavage) into phosphate. Purine nucleoside phosphorylase (PNP) then binds phosphate

Table 1: Leakage Rates: ATP Consumption by the Ybt A Domain with Different Amino Acid Substrates in the Absence of a Thiol Acceptor Cosubstrate[a]

	L-cysteine	*S*-2-aminobutyrate	*β*-Cl-L-Ala
apo-HMWP2 1−1491	0.14	0.35	0.21
holo-HMWP2 1−1491	0.24	0.67	0.45
holo-HMWP2 1−1491 + 5 mM DTT	0.40	0.74	0.70

[a] All rates are per minute, and were measured in the spectrophotometric assay for pyrophosphate release.

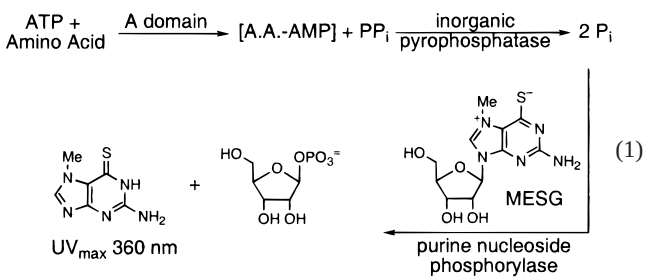

(1)

and uses it to cleave 2-amino-6-mercapto-7-methylpurine ribonucleoside (MESG) into ribose 1-phosphate and 2-amino-6-mercapto-7-methylpurine, which has an absorbance maximum at 360 nm. Increases in A_{360} over time can be related to increases in PP_i production through a standard curve constructed from known PP_i concentrations versus ΔA_{360}. Such a curve gave a molar extinction coefficient (ϵ) of 17 600 $(M\cdot cm)^{-1}$, in good agreement with the 19 500 $(M\cdot cm)^{-1}$ measured previously (*26*). The relationship between A_{360} and PP_i concentration was found to be linear between 0 and 24 μM PP_i.

Rates of ATP usage by apo-HMWP2 1−1491 were then measured using this assay. In the presence of ATP but absence of amino acid, there should be no release of PP_i. However, there was small but measurable ATPase activity ($\sim$1 min^{-1}) which was traced to the protein stocks, and which we ascribed either to a contaminating nonspecific ATPase or to MESG lysis. In the presence of an activatable amino acid but absence of an acceptor cosubstrate (e.g., a holo-PCP domain) for the adenylation domain, HMWP2 1−1491 should only activate the amino acid substrate, and the resulting aminoacyl-AMP should remain tightly bound in the A domain active site. Any net catalytic ATP use in the presence of amino acid substrate indicates that the A domain is losing the activated aa-AMP to adventitious water in the active site or by escape into solution. These data are shown in the first row of Table 1. The apo form of HMWP2 1−1491 consumes ATP at a slow but steady rate of 0.14 min^{-1} in the presence of 5 mM L-cysteine. While this rate increases to 0.35 and 0.21 min^{-1} in the presence of 10 mM *S*-2-aminobutyrate or *β*-chloro-L-alanine, respectively, all three rates are slow, on the order of 600-fold below k_{cat} for ATP−PP_i exchange for the alternate substrates, and 2700-fold below k_{cat} for L-cysteine. First, these results validate the expectation that the thermodynamically activated aa-AMPs are sequestered in this A domain's active site and only slowly dissociate. Second, these slow rates give assurance that higher measured rates of ATP consumption in the presence of a thiol acceptor cosubstrate, reported below, will not be due to unspecific "leakiness" of the A domain.

Amino Acid-Dependent ATP Usage by Holo-HMWP2 1−1491. Since the Ybt A domain is being assayed in the

context of a neighboring PCP1 domain, embedded *in cis* in a downstream location in the 1−1491 fragment of HMWP2 [the shorter 1−1061 fragment failed to support ATP−PP_i exchange (*11*)], rates of ATP usage were also measured for holo-HMWP2 1−1491, with the PCP1 domain phosphopantetheinylated in vitro by Sfp, in the presence of all three amino acids. In these experiments, it was anticipated that the A domain will activate the amino acid, transfer the adenylate to the adjacent PCP1 (Figure 1C), activate another equivalent of amino acid, and then wait, having run out of acceptor substrate to which to transfer. Data are shown in Table 1. Steady-state ATP consumption rates are roughly doubled over apo-HMWP2 1−1491, but are still low overall, with a net ATPase activity of less than one catalytic event per minute per A domain. Assuming that the A domain "leakiness" remains the same in apo- vs holo-enzyme (and is not allosterically increased by assembly line backup), this increase in rate could be ascribed to hydrolysis/thiolysis of the PCP1-attached aminoacyl thioester and subsequent reloading by the A domain. To check whether thiolysis rates, and thereby, ATP usage, could be increased by external thiols, 5 mM dithiothreitol (DTT) was added to another set of these reactions and the PP_i release measured, as shown in Table 1. Rates are again increased, although modestly: DTT can accelerate net ATPase activity over the holo-1−1491 rate by 2-fold for the different amino acid substrates. The acceleration is thus measurable, but DTT has little effect on hydrolysis/thiolysis of PCP-attached thioesters in this system.

Transfer of Activated Amino Acids to Acceptor Cosubstrates: PCP3-TE. Having established ATP consumption in the absence of an acceptor thiol cosubstrate, and in the presence of one (PCP1-P-pant-SH) linked to the A domain *in cis*, we next examined the effect of addition of an HS-P-pant substrate *in trans*. PCP3-TE represents the C-terminal fragment of HMWP1, a natural substrate for HMWP2's adenylation domain. When holo-PCP3-TE was added to HMWP2 1−1491, L-cysteine, and ATP in the spectrophotometric assay, a dramatic acceleration in ATP hydrolysis was observed. By varying the concentration of PCP3-TE, from 0 to 35 μM, Michaelis−Menten kinetics could be measured; kinetics were also determined for *S*-2-aminobutyrate and β-chloro-L-alanine. These data are plotted in Figure 4A. First, the accelerations in ATPase activity are dramatic, with rates of 86−195 min^{-1} at saturation, reflecting more than 100-fold increases over ATPase rates in the absence of holo-PCP3-TE. Second, while there is about a 2-fold difference in the k_{cat} and K_m values among the three amino acid substrates, the catalytic efficiencies (k_{cat}/K_m) are very similar, suggesting that *transfer* kinetics of an activated aminoacyl-AMP to the P-pant-SH of the cognate PCP3 acceptor cosubstrate are largely independent of the identity of the particular amino acid, once it has been converted into the aminoacyl-AMP. A rate of 100−200 min^{-1} may represent the chemical step for this A domain's second half-reaction.

Radioactive Amino Acid Transfer to PCP3-TE. To ensure that the thiol cosubstrate acceleration of the A domain's amino acid-dependent ATPase cleavage rate was indeed reflecting an acceleration of aa-AMP transfer, covalent aminoacylation of PCP3-TE was measured directly. The kinetics of amino acid transfer for HMWP2 1−1491 to PCP3-TE were measured in a [^{35}S]-L-cysteine incorporation

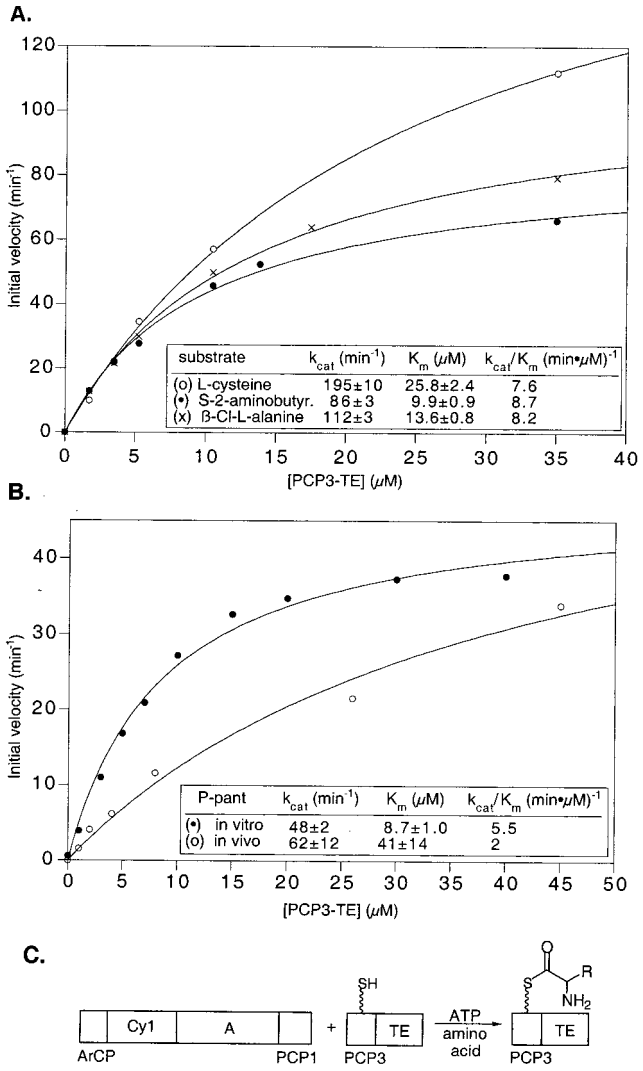

FIGURE 4: Substrate transfer kinetics from HMWP2 1−1491 to PCP3-TE. (A) Transfer kinetics for the three activated amino acids, measured in the pyrophosphate release assay. (B) Transfer kinetics for [^{35}S]-L-Cys, measured in the radioactive incorporation/precipitation assay. The two sets of data points represent holo-PCP3-TE substrate that was phosphopantetheinylated in vitro and in vivo. (C) Schematic of the transfer.

assay, in which the PCP3-TE acquires a covalently attached radioactive amino acid label. Initial velocities of transfer were measured by scintillation counting of TCA-precipitated enzymatic reactions, since the Cys-*S*-P-pant linkage on PCP3-TE is acid-stable. Two sets of reactions were performed: one with purified, holo-PCP3-TE from coexpression of Sfp, and one with in vitro phosphopantetheinylated PCP3-TE (Figure 4B). Because the assay requires [^{35}S]-L-Cys of high specific activity to achieve a good signal in the precipitated [^{35}S]-L-Cys-*S*-PCP3-TE, Cys concentrations of $\leq$100 μM were used, leading to apparent k_{cat} values of 48 min^{-1} (in vitro P-pant) and 61 min^{-1} (in vivo P-pant). For reasons not yet clear, the in vivo phosphopantetheinylation of PCP3-TE gave a K_m of 40 μM for holo-PCP3-TE while the in vitro posttranslational priming of apo- to holo-PCP3-TE gave a K_m of 8.3 μM.

Stoichiometries of Covalent Aminoacylation of Holo-PCP3-TE and HMWP2 1383−2035 (S1977A). To eliminate the possibility that the difference in apparent K_m's measured above arose from different stoichiometries of phosphopan-

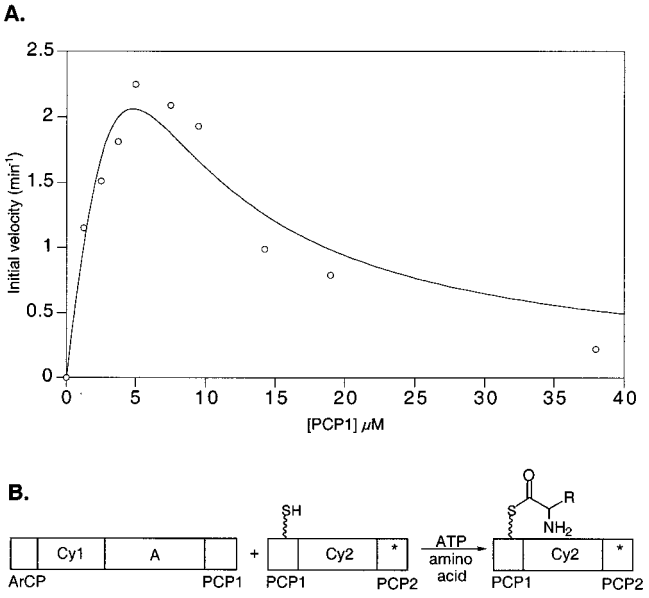

FIGURE 5: (A) L-Cys transfer kinetics from HMWP2 1−1491 to HMWP2 1383−2035 (S1977A), representing PCP1, measured in the pyrophosphate release assay. Severe substrate inhibition above 5 μM was observed. The general substrate inhibition equation (*27*) was used to fit the data points, but only a lower limit for k_{cat} ($\geq$2 min^{-1}) could be determined. This rate is some 50−100-fold below k_{cat} for transfer to PCP3-TE. (B) Schematic of the transfer.

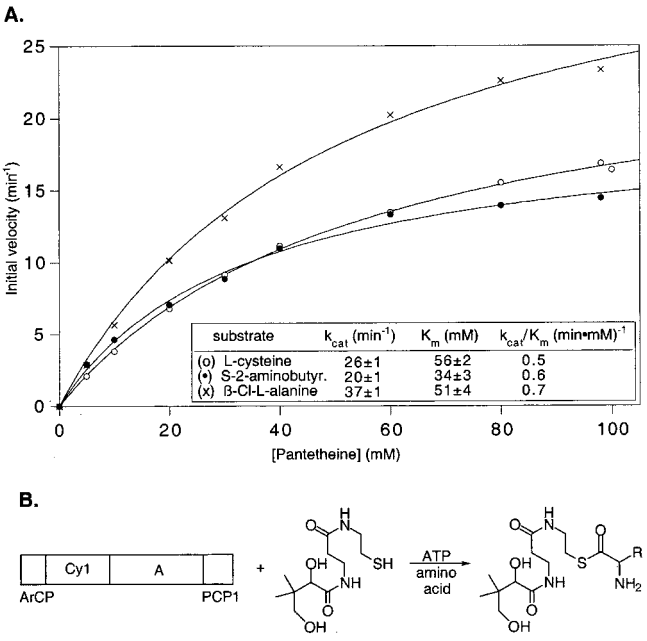

FIGURE 6: Substrate transfer kinetics from HMWP2 1−1491 to pantetheine. (A) Transfer kinetics for the three activated amino acids, measured in the pyrophosphate release assay. Catalytic efficiencies are some 10^4-fold below that observed for PCP3-TE. (B) Schematic of the transfer.

tetheinylation between the in vitro and the in vivo PPTase-treated PCP3-TE, the extent of covalent aminoacylation by HMWP2 1−1491 was measured by [^{35}S]-L-Cys and [1-^{14}C]-L/D-2-aminobutyrate incorporation. For holo-PCP3-TE, stoichiometries of 21% and 32% were calculated for Cys and 2-aminobutyrate, respectively. These values were essentially unchanged (20% and 33%) when the in vivo phosphopantetheinylated PCP3-TE was incubated first with Sfp and CoA, indicating that in vivo phosphopantetheinylation was complete. For comparison, the *in trans* aminoacylation of PCP1 of HMWP2 1383−2035 (S1977A) fragment was also measured, and values of 19% and 30% were obtained.

Transfer of Activated Amino Acids to Acceptor Cosubstrates: HMWP2 1383−2035 (S1977A). The protein fragment HMWP2 1383−2035 (S1977A) encompasses the C-terminal three domains of HMWP2 (PCP1-Cy2-PCP2) in which PCP2 has been inactivated by mutation of the serine attachment point for phosphopantetheine to alanine. This fragment thus presents PCP1 to the A domain only, and was chosen because its wild-type analogue has proven active for biosynthesis of hydroxyphenyl-thiazolyl-thiazolinyl-carboxylate in combination with HMWP2 1−1382 (*12*). In measuring transfer kinetics of L-Cys from HMWP2 1−1491 to this fragment in the PP$_i$ release assay, severe substrate inhibition (*27*) was observed above 5 μM HMWP2 1383−2035 (Figure 5A). A K_m was thus impossible to determine, and a k_{cat} can only be established as $\geq$2 min^{-1}. We do not know why such poor behavior occurs in this combination; the theoretically superior system of HMWP2 1−1382 and 1383−2035 (which does not present the complication of an *in cis* and an *in trans* PCP1) was not tested because of lower activity of 1−1382 in the ATP−PP$_i$ exchange assay relative to the 1−1491 fragment (*12*), perhaps due to lack of the structural contribution of the PCP1 domain.

Transfer of Activated Amino Acids to Acceptor Cosubstrates: Pantetheine and Coenzyme A. To begin to determine how much of the holo-PCP3-TE structure was necessary to observe accelerated transfer of the aminoacyl-AMPs sequestered in the A domain of HMWP2 1−1491, pantetheine and CoA were tested in the same assay as above. Pantetheine and CoA represent different forms of the "prosthetic arm" that constitutes the nucleophilic moiety of the carrier protein domains. The data of Figure 6A show pantetheine was a recognizable mimic of the pantetheinyl arm of holo-PCP3, with accelerations of 30−80-fold (k_{cat} = 20−37 min^{-1}) with the three aminoacyl-AMPs. These k_{cat} values are 3−7-fold below the accelerations effected by PCP3-TE, but at greatly elevated K_m's, about 3000-fold higher. Finally, CoA was tested as a specific thiol cosubstrate in this experiment with L-cysteine; its k_{cat} of 0.9 min^{-1} (Figure 7A) was detectably above the leak rate, but only 3−4-fold above, while the K_m was 10-fold below that of pantetheine. This demonstrates clearly that there is specificity for the surface presenting the pantetheinyl-SH to this A domain.

DISCUSSION

NRPSs assemble their peptide natural products by a thiotemplating process (*13*), in which adenylation domains select and activate amino acid monomers as aminoacyl-AMPs before transferring them to the posttranslationally introduced phosphopantetheine group on adjacent peptidyl carrier protein domains (PCP). Condensation or cyclization domains are then responsible for linking these monomers together, most often in an amide bond, before the mature product is released from the final, most downstream PCP by the C-terminal thioesterase domain. An archetypal NRPS has repeating modules of (-C-A-PCP-)$_n$ domain triads, with each A domain responsible for loading its adjacent PCP with the correct monomer and each C domain acting to link the growing chain on the upstream PCP with the monomer on the downstream PCP. In such a system, PCP acylation (by

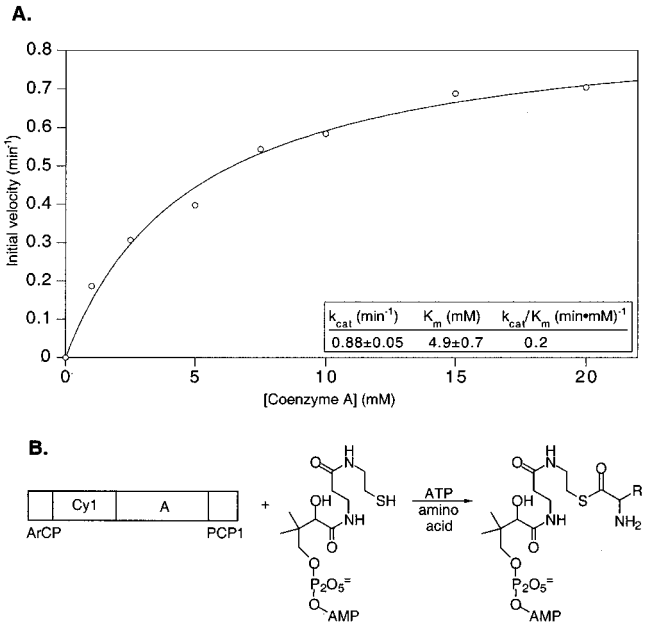

FIGURE 7: (A) L-Cys transfer kinetics from HMWP2 1−1491 to CoA, measured in the pyrophosphate release assay. Catalytic efficiency is some 4×10^4-fold below that observed for PCP3-TE. (B) Schematic of the transfer.

aminoacyl and/or peptidyl chains) is intramolecular and stoichiometric and thus difficult to evaluate for rate and specificity.

In light of this, the two central proteins, HMWP2 and HMWP1, of yersiniabactin synthetase present an intriguing architecture for study of PCP aminoacylation. PCP1 is located immediately downstream of the single adenylation domain (residues 545−1382), PCP2 is *in cis* with the A domain but is separated by two domains, while PCP3 is on the separate protein HMWP1. While it has been demonstrated previously that HMWP2 1−1491 can load [^{35}S]-L-cysteine on the 10 kDa PCP1 and PCP3 excised protein fragments *in trans* (*10, 11*), there have been no experiments on the kinetics of this system. This study examines both the amino acid substrate specificity of this adenylation domain and also its rate and specificity for transfer of the aminoacyl group to various thiol substrates.

To test the specificity of the A domain in its first half-reaction for amino acid substrates, a number of proteinogenic and nonproteinogenic amino acids were tested for their ability to support ATP−PP_i exchange. It has been previously reported that L-cysteine is the natural substrate and the L-serine is not accepted (*11*). We found that while nine analogues of Cys were inactive, two additional amino acids were active in this reaction: *S*-2-aminobutyrate and β-chloro-L-alanine (Figure 3), while L-serine yielded a very weak, but positive signal (data not shown). Structurally, 2-aminobutyrate and β-chloroalanine replace the thiol of cysteine with a methyl group or a chlorine atom, respectively. In an earlier study of the cysteine adenylating domain of the fungal NRPS enzyme ACV synthetase, which makes the tripeptide precursor to penicillin, a number of cysteine analogues were active for ATP−PP_i exchange (*28*), but β-chloro-L-alanine is the only amino acid active in both ACV and Ybt A_{Cys} domains. The catalytic efficiencies of *S*-2-aminobutyrate and β-chloro-L-alanine for Ybt A domain-catalyzed ATP−PP_i exchange were down by approximately 40- and 10-fold, respectively, relative to L-cysteine. Although k_{cat} values were not reported for the ATP−PP_i exchange reaction of the ACV synthetase A_{Cys} domain, apparent K_m's of 0.21 mM for cysteine, 0.8 mM for L-allylglycine, and 2.8 mM for L-vinylglycine (*28*) can be compared favorably to the values for the Ybt A domain in Figure 3. As noted above, neither L-allylglycine nor L-vinylglycine were substrates for the Ybt A domain. It should also be noted that even though *S*-2-aminobutyrate and β-chloro-L-alanine are readily activated, neither would present competition for cysteine in vivo.

The continuous, coupled enzyme assay used here to measure pyrophosphate release as a proxy for ATP consumption during amino acid activation and transfer was originally developed to measure inorganic phosphate (*21*), but has also been applied to pyrophosphate release (*25*), in particular the activity of aminoacyl-tRNA synthetases (*26*). We first applied this assay to amino acid-dependent ATP consumption by the adenylation domain in the absence of a P-pant-SH acceptor cosubstrate. We found very low rates of "leakage" of the aminoacyl-AMP across the three substrates (Table 1), indicating that the adenylation domain is quite good at retaining the bound intermediate and that ATP cleavage is tightly coupled to the two-step process of substrate activation and transfer. [The structural basis for aa-AMP binding has been examined in the context of the published crystal structure of the Phe-activating A domain of gramicidin-S synthetase (*17, 29*).] Substrate activation by the enterobactin synthetase system has also been examined (*30*), and it was found that leakage rates for EntE [2,3-dihydroxybenzoate (DHB) activating] are 10-fold higher for salicylate than for DHB. Notable in the Ybt system is the only modest increase in leakage rates for alternate substrates, in contrast to EntE; EntE appears to retain its unnatural substrates less well than HMWP2 does. Studies on the leakage rates of HMWP2 1−1491 as compared to those of the full-length, 230 kDa protein await purification of the latter.

Additional leakage rates have been measured for the intact trimodular ACV synthetase of *Acremonium chrysogenum*, a 420 kDa NRPS (*31*). The basal rate of ATPase activity (no amino acid substrate) was reported as 0.7 min^{-1}, and single additions of aminoadipate (0.8 min^{-1}), cysteine (2.6 min^{-1}), and valine (1.8 min^{-1}) show similar low leakage rates of the bound aminoacyl-AMPs. The net Cys-dependent ATPase rate of 1.9 min^{-1} for the A_{Cys} domain of ACV synthetase is roughly 10-fold higher than the analogous Cys-dependent rates for the Ybt A domain (Table 1).

Examination of holo- vs apo-HMWP2 1−1491 allowed evaluation of the effect of a stoichiometric amount of *in cis* P-pant-SH acceptor [on the PCP1 domain (Figure 1C)] on rates of aa-AMP transfer from the A domain (Table 1). This holo-enzyme should stoichiometrically load the adjacent PCP1 (*11*), but after this initial burst of ATP consumption (not measured here), steady-state PP_i release should return to the amino acid-dependent leakage rate. The 2-fold increase in ATP hydrolysis that we measure could be attributed to a slow hydrolysis of the PCP1-aminoacyl thioester and subsequent reloading or to some doubling of the leakage rate of aa-AMP from the adjacent A domain in solution. This rate was increased another 2-fold upon addition of 5 mM DTT, but again, the absolute rates are low, under 1 min^{-1}. These results indicate that hydrolysis or thiolysis does not

contribute significantly to ATP consumption and that the aa-AMPs are effectively sequestered from bulk solvent and from nonspecific thiols. In contrast, it was reported for ACV synthetase that added DTT (8 mM) "significantly" increased ATP consumption (*31*). Measurement of the *in cis* rate of aa-AMP transfer to the P-pant-SH moiety of PCP1 will require rapid quench methods as it is complete within a few seconds (data not shown).

With these rates of ATP consumption for apo- and holo-HMWP2 1−1491 established, we turned to *in trans* HS-P-pant acceptor cosubstrates. PCP3-TE, a 40 kDa fragment of the 350 kDa HMWP1, which is naturally loaded *in trans* by HMWP2, dramatically increased ATP turnover in the assay. By measuring initial velocities as a function of PCP3-TE concentration, Michaelis−Menten kinetics for PCP3-TE were measured with all three amino acid substrates, establishing saturation and specific recognition of P-pant-SH in the PCP3 context with a K_m of 10−26 μM (Figure 4A). At saturation, the cysteinyl, β-chloroalanyl, and 2-aminobutyryl transfers were within 2−3-fold (86−195 min^{-1}), a very small range for these three different amino acids. These measurements of both steps of an A domain's catalytic activities, aminoacyl-AMP ligation and then aa-AMP transfer, indicate that selectivity in NRPS monomer activation and loading occurs in the choice of amino acid in step 1 by the adenylation domain, and the identity of the acceptor substrate in step 2, but is independent of the amino acid adenylate in this second step. If this is generalizable to other A domains of NRPSs, it would suggest only minimal editing and fidelity controls after aa-AMP formation, in contrast to some of the AARS. For example, both the Val-RS and the Ile-RS can activate incorrect amino acids (Thr and Val) as their adenylates, albeit at lower catalytic efficiencies that for their natural substrates. However, both possess editing functions that hydrolyze the misacylated Thr-$tRNA^{Val}$ or the misactivated Val-AMP, respectively, in the presence of their cognate tRNAs, and thus dramatically lower the rate of misincorporation into proteins (*19, 20*). Both of these editing functions trade unproductive ATP consumption for higher accuracy. In essence, Val-RS and Ile-RS become ATP hydrolases in the presence of their cognate tRNAs and an incorrect, alternate amino acid. In the Ybt system, given that both the natural Cys-AMP and the misacylated β-chloro-Ala-AMP and 2-aminobutyryl-AMP are released/hydrolytically edited at the same slow rates in both apo- and holo-HMWP2 1−1491, this argues *against* fidelity checks after aa-AMP ligation both in the A domain active site and during second-step transfer to the HS-P-pant moiety of PCP1. If there were editing of misactivated or misacylated substrates by the A domain, one would expect to observe significantly higher ATP hydrolysis rates by holo-HMWP2 1−1491 in the presence of β-Cl-Ala and 2-aminobutyrate. For comparison, the cysteinyl-tRNA synthetase also catalyzes ATP−PP_i exchange in the presence of 2-aminobutyrate, but the relative k_{cat}/K_m is 3×10^{-6} of the value for cysteine. Notably, Cys-RS lacks an editing function because it does not have a close competitor for binding in vivo (*32*).

The amino acid and PCP3-TE acceptor cosubstrate dependencies for A domain *catalytic* hydrolysis of ATP to AMP and PP_i reported above are interpreted as evidence for multiple cycles of aa-AMP formation and *transfer* by the A domain to the P-pant thiol on PCP3. This transfer was validated in two ways. First, the stoichiometries of aminoacylation by [^{35}S]-L-Cys and by [1-^{14}C]-L/D-2-aminobutyrate were measured. The A domain was able to achieve loading stoichiometries of 21% and 32% for these two substrates for PCP3-TE. Exposure of in vivo phosphopantetheinylated PCP3-TE to an additional Sfp and CoA in vitro did not change these stoichiometries significantly (20% and 33%, respectively), indicating that coexpression of Sfp reliably yields holo-PCP3-TE. Very similar aminoacylation stoichiometries (19% and 30% by [^{35}S]-L-Cys and by [1-^{14}C]-L/D-2-aminobutyrate, respectively) were obtained for the *in trans* modification of PCP1 of HMWP2 1383−2035 (S1977A) fragment. Why these loading stoichiometries vary and do not reach 100% is unclear, but the data do demonstrate that covalent loading of both a natural and an unnatural amino acid substrate is possible. Second, aminoacyl-*S*-PCP3 formation was established with the rates of transfer of [^{35}S]-L-Cys (Figure 4B). Rates of 50−60 min^{-1} are lower than the rates of 86−195 min^{-1} measured in the PP_i release assay. While these could reflect some significant diversion of the increased aa-AMP release flux to water rather than to PCP3-TE (i.e., an uncoupling of ATPase activity from aminoacyl-*S*-PCP formation), it is more likely that the 50−60 min^{-1} rates, measured with [^{35}S]-L-Cys, ~100 μM, are subsaturating (K_m for Cys = 650 μM) and the true k_{cat} for aa-AMP transfer is thus underestimated in the radioactive incorporation assays. The preferred substrate for testing the specificity of rate acceleration in the PP_i release assay is apo-PCP3-TE; however, we have found (Z.S. and C.T.W., unpublished observations) that during *E. coli* expression some percentage of apo-protein is phosphopantetheinylated by native PPTases, and thus rigorously apo-carrier protein domains are difficult to obtain.

The poor behavior of HMWP2 1383−2035 (S1977A), a PCP1 construct, is in contrast to that of PCP3-TE. The former exhibited severe substrate inhibition in the PP_i release assay (Figure 5A), such that a K_m could not be determined and only a lower limit (2 min^{-1}) could be set for k_{cat}. [Similar substrate inhibition has been noted earlier in the PPTase-catalyzed phosphopantetheinylation of various PCPs (*8, 22, 33*).] The reasons for this are unclear; it is possibly an artifactual consequence of the presence of another unit of PCP1 on the 1−1491 fragment, or of the *in trans* interaction of two domains (A and PCP1) that normally interact *in cis*. A more desirable A domain fragment (1−1382) that does not have PCP1 *in cis* was not used because of inferior activity. The conclusion that can be drawn, however, is that the A domain clearly differentiates between holo-PCPs in the kinetics of aminoacyl transfer.

We then turned to the specificity for recognition of the HS-pantetheinyl arm that is used to capture the aa-AMPs bound in the A domain. First, one can look at free pantetheine vs the pantetheinyl-containing coenzyme A. Pantetheine is the dephospho arm of a holo-PCP while CoA-SH has a 3′,5′-ADP instead of the P-pant-Ser-PCP. When pantetheine was tested as a substrate for HMWP2 1−1491, k_{cat} values for transfer were up 30-fold, and saturation was detected although binding was poor with K_m's of 34−56 mM (Figure 6A). Fixing the pantetheinyl arm on its natural PCP3 domain cosubstrate lowered K_m's by 3 orders of magnitude, demonstrating a dramatically improved recognition for P-pant presentation by a folded carrier protein domain. The k_{cat}

values for PCP3-TE were up 3−7-fold over pantetheine, and the 195 min^{-1} for L-Cys may be a limiting value for the Cys-AMP capture by the thiol of the P-pant prosthetic group. When CoA was tested, it was only 4-fold above background for Cys-AMP release, 25-fold below pantetheine, and 200-fold below PCP3-TE transfer rates (Figure 7A). Since the thiol reactivity for all three cosubstrates is equivalent, the 3′,5′-ADP moiety of CoA must present an electrostatic or steric impediment to transfer. The net effect of anchoring the P-pant thiol to a specific PCP rather than to 3′,5′-ADP is a factor of 10^4 in catalytic efficiency (10^2 in both k_{cat} and K_m). Given a second example of differential recognition of homologous and heterologous PCP domains *in trans* by EntE from enterobactin synthetase (*30*), this suggests that pairs of A-PCP domains may have evolved for optimized recognition and P-pant capture of peptidyl-, aminoacyl-, and acyl-AMP intermediates. This may have the practical consequence that reengineering of NRPSs for combinatorial biosynthesis should focus on pairs of A-PCP domains rather than individual swaps of either domain.

How a properly anchored P-pant thiol pries its way into an A domain active site with selective recognition and chemical acceleration of aa-AMP capture remains to be determined and could be as direct as penetration through a channel to the A domain active site by the 20 Å long P-pant arm, or could involve an allosteric component, e.g., a conformational change brought about by PCP-mediated protein−protein interaction. Recent publications have shown that CoA and pantetheine could capture aa-AMPs sequestered in active sites of tRNA synthetases (*34*), but rates of capture were variable and slow, and it is as yet unclear what fraction of that capture is scavenging of aa-AMPs slowing leaking into solution, as opposed to a specific, and perhaps vestigial, binding site for a pantetheinyl arm.

In summary, the covalent aminoacylation of holo-carrier domains in NRPS appears to involve two levels of A domain specificity: first, amino acid selection for activation as the aminoacyl adenylate; and second, transfer of the adenylate to a phosphopantetheinyl thiol on a specific PCP. Unlike some AARSs, we found no evidence for an editing mechanism in the Ybt A domain; unnatural activated substrates do not induce a higher ATP hydrolysis rate than the natural L-cysteine, nor are there appreciable differences among the transfer rates of the three substrates accepted by the A domain. The A domain can also transfer to pantetheine and coenzyme A, but at much lower catalytic efficiencies, indicating that attachment of the P-pant arm on a specific PCP is critical for efficient aminoacylation.

ACKNOWLEDGMENT

We thank Deborah A. Miller for providing the HMWP2 1383-2035 (S1977A) protein fragment, Luis E. N. Quadri for purified Sfp, and Torsten Stachelhaus for a careful reading of the manuscript.

REFERENCES

1. Marahiel, M. A., Stachelhaus, T., and Mootz, H. D. (1997) *Chem. Rev. 97*, 2651−2673.
2. von Döhren, H., Keller, U., Vater, J., and Zocher, R. (1997) *Chem. Rev. 97*, 2675−2705.
3. Konz, D., and Marahiel, M. A. (1999) *Chem. Biol. 6*, R39−R48.
4. Konz, D., Klens, A., Schörgendorfer, K., and Marahiel, M. A. (1997) *Chem. Biol. 4*, 927−937.
5. Byford, M. F., Baldwin, J. E., Shiau, C.-Y., and Schofield, C. J. (1997) *Chem. Rev. 97*, 2631−2649.
6. van Wageningen, A. M. A., Kirkpatrick, P. N., Williams, D. H., Harris, B. R., Kershaw, J. K., Lennard, N. J., Jones, M., Jones, S. J. M., and Solenberg, P. J. (1998) *Chem. Biol. 5*, 155−162.
7. Gehring, A. M., Mori, I., and Walsh, C. T. (1998) *Biochemistry 37*, 2648−2659.
8. Quadri, L. E. N., Sello, J., Keating, T. A., Weinreb, P. H., and Walsh, C. T. (1998) *Chem. Biol. 5*, 631−645.
9. Quadri, L. E. N., Keating, T. A., Patel, H. M., and Walsh, C. T. (1999) *Biochemistry 38*, 14941−14954.
10. Gehring, A. M., DeMoll, E., Fetherston, J. D., Mori, I., Mayhew, G. F., Blattner, F. R., Walsh, C. T., and Perry, R. D. (1998) *Chem. Biol. 5*, 573−586.
11. Gehring, A. M., Mori, I., Perry, R. D., and Walsh, C. T. (1998) *Biochemistry 37*, 11637−11650.
12. Suo, Z., Walsh, C. T., and Miller, D. A. (1999) *Biochemistry 38*, 14023−14035.
13. Stein, T., Vater, J., Kruft, V., Otto, A., Wittmann-Liebold, B., Franke, P., Panico, M., McDowell, R., and Morris, H. R. (1996) *J. Biol. Chem. 271*, 15428−15435.
14. Lambalot, R. H., Gehring, A. M., Flugel, R. S., Zuber, P., LaCelle, M., Marahiel, M. A., Reid, R., Khosla, C., and Walsh, C. T. (1996) *Chem. Biol. 3*, 923−936.
15. Keating, T. A., and Walsh, C. T. (1999) *Curr. Opin. Chem. Biol. 3*, 598−606.
16. Cane, D. E., Walsh, C. T., and Khosla, C. (1998) *Science 282*, 63−68.
17. Stachelhaus, T., Mootz, H. D., and Marahiel, M. A. (1999) *Chem. Biol. 6*, 493−505.
18. Fersht, A. (1985) *Enzyme Structure and Mechanism*, 2nd ed., W. H. Freeman, New York.
19. Fersht, A. R. (1977) *Biochemistry 16*, 1025.
20. Fersht, A. R., and Dingwall, C. (1979) *Biochemistry 18*, 1238−1245.
21. Webb, M. R. (1992) *Proc. Natl. Acad. Sci. U.S.A. 89*, 4884−4887.
22. Quadri, L. E. N., Weinreb, P. H., Lei, M., Nakano, M. M., Zuber, P., and Walsh, C. T. (1998) *Biochemistry 37*, 1585−1595.
23. Sambrook, J., Fritsch, E. F., and Maniatis, T. (1989) *Molecular Cloning: A Laboratory Manual*, 2nd ed., Cold Spring Harbor Laboratory Press, Plainview, NY.
24. Pavela-Vrancic, M., Dieckmann, R., von Döhren, H., and Kleinkauf, H. (1999) *Biochem. J. 342*, 715−719.
25. Upson, R. H., Haugland, R. P., Malekzadeh, M. N., and Haugland, R. P. (1996) *Anal. Biochem. 243*, 41−45.
26. Lloyd, A. J., Thomann, H.-U., Ibba, M., and Söll, D. (1995) *Nucleic Acids Res. 23*, 2886−2892.
27. Cleland, W. W. (1970) in *The Enzymes* (Boyer, P., Ed.) pp 1−65, Academic Press, New York.
28. Baldwin, J. E., Shiau, C.-Y., Byford, M. F., and Schofield, C. J. (1994) *Biochem. J. 301*, 367−372.
29. Conti, E., Stachelhaus, T., Marahiel, M. A., and Brick, P. (1997) *EMBO J. 16*, 4174−4183.
30. Ehmann, D. E., Shaw-Reid, C. A., Losey, H. C., and Walsh, C. T. (2000) *Proc. Natl. Acad. Sci. U.S.A.* (in press).
31. Kallow, W., von Döhren, H., and Kleinkauf, H. (1998) *Biochemistry 37*, 5947−5952.
32. Fersht, A. R., and Dingwall, C. (1979) *Biochemistry 18*, 1245−1249.
33. Gehring, A. M., Bradley, K. A., and Walsh, C. T. (1997) *Biochemistry 36*, 8495−8503.
34. Jakubowski, H. (1998) *Biochemistry 37*, 5147−5153.

BI992341Z